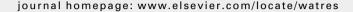


Available at www.sciencedirect.com







Investigation on removal of hardness ions by capacitive deionization (CDI) for water softening applications

Seok-Jun Seo^a, Hongrae Jeon^a, Jae Kwang Lee^a, Gha-Young Kim^a, Daewook Park^b, Hideo Nojima^b, Jaeyoung Lee^{a,*}, Seung-Hyeon Moon^a

ARTICLE INFO

Article history:
Received 6 July 2009
Received in revised form
22 September 2009
Accepted 18 October 2009
Available online 22 October 2009

Keywords:
Capacitive deionization (CDI)
Electrosorption
Hardness ion
Water softening
Activated carbon electrode

ABSTRACT

Capacitive deionization (CDI) for removal of water hardness was investigated for water softening applications. In order to examine the wettability and pore structure of the activated carbon cloth and composites electrodes, surface morphological and electrochemical characteristics were observed. The highly wettable electrode surface exhibited faster adsorption/desorption of ions in a continuous treatment system. In addition, the stack as well as unit cell operations were performed to investigate preferential removal of the hardness ions, showing higher selectivity of divalent ions rather than that of the monovalent ion. Interestingly, competitive substitution was observed in which the adsorbed Na ions were replaced by more strongly adsorptive Ca and Mg ions. The preferential removal of divalent ions was explained in terms of ion selectivity and pore characteristics in electrodes. Finally, optimal pore size and structure of carbon electrodes for efficient removal of divalent ions were extensively discussed.

© 2009 Elsevier Ltd. All rights reserved.

1. Introduction

Purification of several contaminants in tap, ground, and river water is needed for the drinking and industrial purposes. Among the contaminants, hard water minerals such as calcium, magnesium, iron, and manganese ions can react with soap anions, decreasing the cleaning efficiency (Park et al., 2007a). The minerals also induce scaling problems and serious failures in pipelines of boilers, heat exchangers, and electrical appliances such as washing machines, dishwashers and steam irons (Gabrielli et al., 2006).

In order to remove the divalent ions, various methods have been widely applied as a means of effective water softening: chemical precipitation, ion exchange process, nanofiltration, reverse osmosis, and electromembrane systems such as electrodialysis, electrodialysis reversal, and electro-deionization reversal. However, in case of the chemical precipitation, the choices of additional chemicals are restricted for the purpose of drinking water. Monovalent ions and acids released in the regeneration of ion exchange and membrane processes would result in harmful effects on environment. Finally, high power consumption and expenses are required for operation and maintenance of the equipment (Čuda et al.,

^a Department of Environmental Science and Engineering, Gwangju Institute of Science and Technology (GIST), 261 Cheomdan-gwagiro, Buk-gu, Gwangju 500-712, Republic of Korea

^b Advanced R&D Group, Digital Appliances Division, Digital Media Business, Samsung Electronics Co., Ltd., 416 Maetan-3dong, Yeongtong-gu, Suwon 443-742, Republic of Korea

^{*} Corresponding author. Tel.: +82 62 970 2440; fax: +82 62 970 2434. E-mail address: jaeyoung@gist.ac.kr (J. Lee).

2006; Gabrielli et al., 2006; Ghizellaoui et al., 2005; Park et al., 2007a). Thus, a cost-effective and low energy consuming electrochemical method has been forced on water softening process.

Capacitive deionization (CDI) is an attractive environmentally-friendly technology for removal of hardness ions consuming relatively small energy, and it does not require any secondary regeneration wastes, expensive membranes, and high pressure pumps. In a configuration of CDI cells, the feed solution flows between each pair of high capacity electrodes, i.e., porous carbon electrodes. By polarizing both electrodes, the charged ions are adsorbed on each electrode surface; positively charged ions are attracted on a surface of the negatively charged electrode and vice versa (Ahn et al., 2007; Farmer et al., 1996; Zou et al., 2008).

Although numerous previous studies have been contributed on desalination of monovalent ions, few researchers have concentrated on water softening using CDI (Lee et al., 2006; Oren, 2008; Welgemoed and Schutte, 2005). Gabelich et al. showed that monovalent ions are preferentially removed rather than divalent ions in the case of carbon aerogel electrodes (Gabelich et al., 2002). On the other hand, different observations have also been reported while others revealed opposite trends (Johnson and Newman, 1971; Xu et al., 2008). Therefore, systematic investigations on the selective removal of divalent ions using CDI are needed for the water softening applications.

In this study, two types of activated carbon electrodes were compared in terms of surface morphological and electrochemical properties to investigate effects of the wettability and pore structure on the removal characteristics of divalent cations. The selective removal efficiency of hardness ions in the CDI process was extensively discussed and prospective features of appropriate electrode were proposed for water softening applications.

2. Experiments

2.1. Materials

The activated carbon cloth (AC cloth) electrode was provided by Kuraray Chemical (Japan) and the activated carbon composites (AC composites) by Material Methods (USA). The artificial feed solution was prepared by dissolving 288 mg/L of CaCl₂, 220 mg/L of MgSO₄ · 7 H₂O, and 390 mg/L of NaHCO₃ (Aldrich, USA) in D.I. water. The feed solution was used for all the experiments in this research and its total hardness and conductivity were 350 ppm (as CaCO₃) and 1000 μS cm $^{-1}$, respectively.

2.2. Operational configuration

Two sizes of unit cells (effective area of each cell is 25 and 100 cm², respectively) and a five-cell stack (each cell: 100 cm²) were designed to conduct a comparison study of CDI performance with different types of carbon electrodes (Fig. 1). The unit cell in which carbon electrodes are employed is divided into two parallel compartments and a spacer was positioned between the electrodes to ensure flow rates and polarization

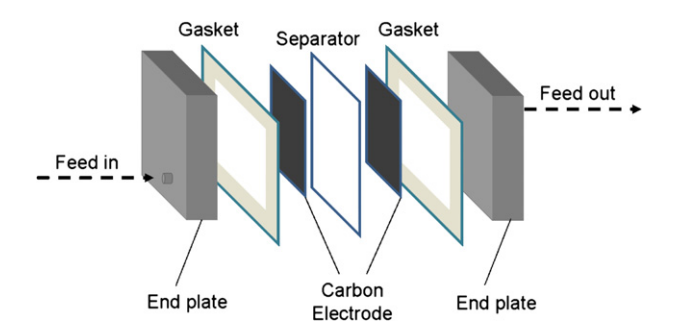


Fig. 1 - Schematic diagram of a CDI unit cell.

between the two compartments. Graphite current collectors were physically attached to apply a voltage using power supply. For the voltage applying at 1.5 V, a DC power supply was provided by Agilent® (6613C, USA) and it was connected to each end plate. The prepared feed solution was injected into the unit cell by a Cole–Parmer Masterflex® pump (Barrington, IL). The effluent of the system was analyzed by using the ion chromatography (DX-120, DIONEX, USA) and conductivity meter (Cole–Parmer, USA). In order to consider feasibility of water softening using CDI, 80% removal of divalent ions was adopted as an optimum goal in unit cell tests.

2.3. Surface analysis

Surface analysis was studied by scanning electron microscope (SEM, S-4700, Hitachi, Japan), energy dispersive X-ray spectrometry (EDX), and the surface condition was characterized by X-ray diffraction (XRD, Rigaku, D/MAX Ultima III) XRD. Binding energy of each carbon electrode was observed using the X-ray photoelectron spectroscopy (XPS, Multilab 2000).

In order to measure the hydrophilicity of each electrode depending on the feed solution and D.I. water, the sessile drop method of a Standard Goniometer with Dropimage was used. For a determination of the contact angle, the captured images were analyzed using a DROP image standard software.

The physical adsorption properties were examined by Micromeritics ASAP 2020 (Norcross, GA). The Brunauer–Emmet–Teller (BET) surface area and pore size distribution (PSD) were examined in the condition of nitrogen at 77 K. The PSD was analyzed by the density functional theory (DFT) (Seaton et al., 1989).

2.4. Electrochemical analysis

In order to measure the capacitance of each electrode, cyclic voltammetry (CV) consists of three electrodes cell system and was performed using the AutoLab PGSTAT 30 (Eco Chemie, Netherland). The carbon electrode as a working electrode was immersed in the feed solution for CV measurement. An Ag/ AgCl, sat'd KCl electrode and Pt/Ti plate was used as a reference and counter electrode, respectively. The potential was swept between -1 and $1\,\mathrm{V}$ with scan rates between 1 and $100\,\mathrm{mV}\,\mathrm{s}^{-1}$. The impedances of the unit cell were measured by using the AutoLab with the frequency response analyzer (FRA). The sweep range was from $100\,\mathrm{kHz}$ to $10\,\mathrm{mHz}$ with an amplitude of 5 mV.

3. Results and discussion

3.1. Electrode characterizations

The surface morphologies of the electrodes are shown in Figs. 2a–d. The AC cloth type electrode has closely woven morphology with fibrils of 10–15 μ m diameters, while the AC composite type has a relatively plain surface (Figs. 2a,b). With more enlarged images, the AC cloth type showed a uniform surface with small pores of 10–20 nm diameter, while the AC composite type contained the agglomerated small and large particles (Figs. 2c,d). The surface chemical compositions were analyzed by SEM-EDX (Supplemental Information, Table S1). The AC composites type showed a fluorine element, which results from the added binders such as poly(tetrafluoroethylene) (PTFE) and poly(vinylidene fluoride) (PVDF) to form the electrodes (Park et al., 2007b).

The XPS analysis was carried out to examine elemental compositions of the electrode surfaces (Supplemental Information, Fig. S1a). The XPS spectra showed representative two peaks. The peak at 284.5 eV is a carbon element and the latter

one corresponds to a Teflon binder in carbon electrode (Schulze et al., 2002). The characteristics peak of a fluorine series binder was observed in case of the AC composites type electrodes. In the same manner, the XRD spectra also showed a fluorine series peak at near 18.1° (JCPDS 47-2217) with the AC composites type electrodes (Supplemental Information, Fig. S1b).

In order to examine wettability of each electrode, contact angles were measured using D.I. water and the prepared feed solution. As shown in Fig. 2e, the AC cloth type electrodes had high wettability to absorb those solutions in a short time, thus no droplet formed at the electrode surface. It is known that hydrophilicity of the carbon with functional groups such as carboxyl, carbonyl, and hydroxyl groups enhances its wettability (Ahn et al., 2007; Zou et al., 2008). In addition, the closely woven structure of the fibers that affects a capillary phenomenon would be one of the responsibilities of the good wettability. However, the AC composites electrode (Fig. 2f) formed a droplet of a high contact angle about 140° at the electrode surface regardless of the solution types. This high contact angle is mainly due to hydrophobicity of the AC composites electrode composed of the fluorine series binders, resulting in relatively low wettability compared to the AC cloth. In the CDI

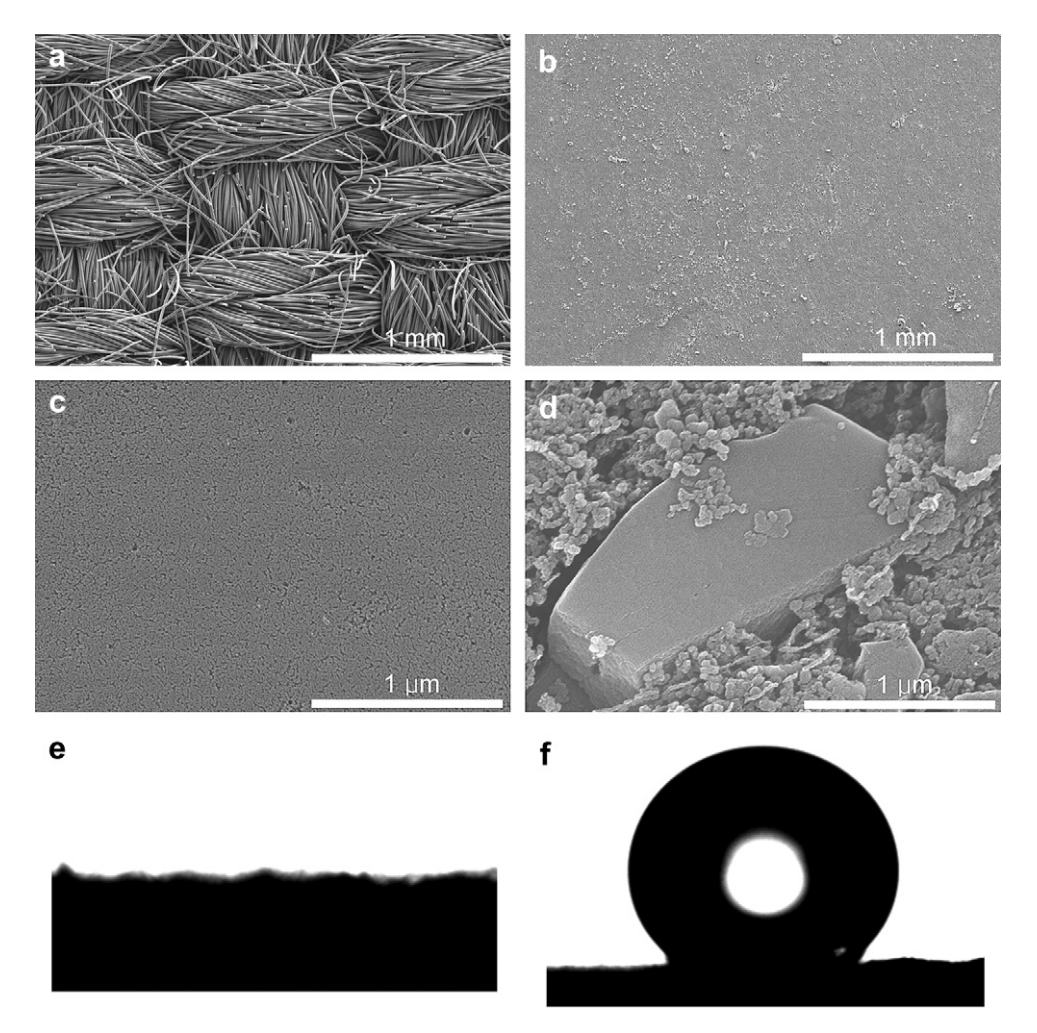


Fig. 2 – Representative SEM images $(50\times)$ of (a) AC cloth and (b) AC composites electrodes. Enlarged images $(50,000\times)$ of (c) AC cloth and (d) AC composites electrodes. Contact angles of the (e) AC cloth and (f) AC composites electrodes measured with the feed solution.

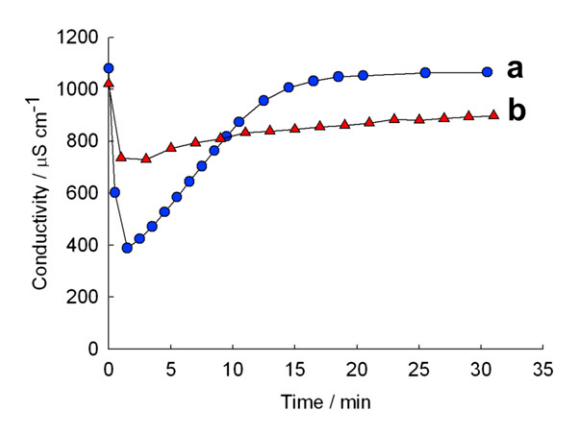


Fig. 3 – Conductivity removal trends depending on electrode types: AC cloth (a) and AC composites (b). The applied voltage was 1.5 V with a flow rate of 4 mL min⁻¹. The apparent surface area of each compartment was 25 cm².

system, thus, the wettability is of importance because it affects total areas for adsorption and removal rate of ions during treatment.

Ion removal characteristics depending on each electrode type are shown in Fig. 3. Ions in the feed solution are adsorbed on the surface of electrodes by employing a voltage to the cell and thus, the product solution exhibits a relatively low conductivity due to the lowered ion concentration. The apparent electrode area of each compartment was 25 cm² and the feed solution was applied to the unit cell with a flow rate of 4 ml min⁻¹. In case of the AC cloth type electrode (Fig. 3a), the conductivity of product solution during the operation rapidly decreased to 35% of the initial value in 2 min, and then completely recovered to the initial value after 15 min. It is understood that adsorbable electrical double layers are getting occupied by ions and the ion removal efficiency became lower.

In case of the AC composites electrode (Fig. 3b), removal kinetics of ions is slower compared to that of the carbon cloth. The conductivity of the treated solution is almost 70% even though the solution was treated for 5 min. Two types of electrodes showed different patterns in adsorption of ions. These differences in removal rate and efficiency might result from wettability of each electrode. In addition, the BET surface area and characteristics of pore structure are important in which diffusion and migration of ions are hindered.

The specific surface areas of the AC cloth and AC composites electrodes were obtained from the BET measurement. As

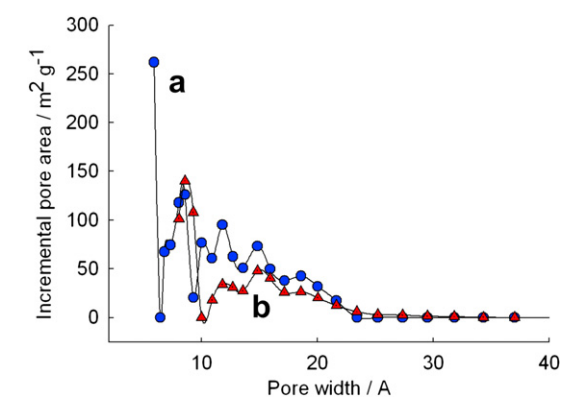


Fig. 4 – Pore size distribution of the AC cloth (●) and AC composites (▲) type electrodes.

shown in Table 1, the AC cloth has a higher specific surface area and more micropore than the AC composites. Although all electrodes exhibited high surface areas above 1000 m 2 g $^{-1}$, it was reported that only a small portion of surface coverage (about 50 m 2 g $^{-1}$) is active for ionic adsorption on carbon aerogel electrodes (Gabelich et al., 2002). Therefore, it is regarded that efforts to make an electrode with high surface areas are still not essential.

PSD analysis in Fig. 4 shows that most of the pores are placed between 0.7 and 2 nm ranges.

Electrochemical characteristics of each electrode were investigated using cyclic voltammetry (Supplemental Information, Fig. S2). Table 2 shows specific capacitances of AC cloth and AC composites applying scan rates of 1 and $100~\text{mV s}^{-1}$. The results indicate the pore characteristics of each electrode.

At the low scan rate of 1 mV s⁻¹ (Fig. S2a), the AC cloth showed 3.5 times higher capacitance than AC composite and it is due to a more microporous area (see Table 1). The capacitance at a low scan rate corresponds to the total capacitance of micropore and mesopore. At the low scan rate, a charging process inside the pore is equilibrated, effectively forming electrical double layers in both micropore and mesopore (Yang et al., 2003). Thus, the ions are electrically adsorbed inside the layers of the micropore as well as the mesopore.

In contrast, at the high scan rate of 100 mV s^{-1} (Fig. S2b), the AC composites electrode showed about six times higher capacitance than that of the AC cloth. This higher capacitance at the higher scan rate is mainly due to the rapid accessibilities

Table 1 – BET surface area of each electrode: AC cloth and AC composites types.

AG composites types	•	
	AC cloth	AC composites
Micropore (<2 nm) Mesopore (2–50 nm) Surface area (m² g ⁻¹)	1349 (m ² g ⁻¹) 461 (m ² g ⁻¹) 1810 (m ² g ⁻¹)	756 (m ² g ⁻¹) 418 (m ² g ⁻¹) 1175 (m ² g ⁻¹)
Micro/BET	0.75	0.64

Table 2 – Specific capacitance of the AC cloth and AC composites electrodes depending on scan rates: 1 and 100 mV s^{-1}

Scan rate (mV s ⁻¹)	Specific ca	Specific capacitance (F g ⁻¹)	
	AC cloth	AC composites	
1	41.5	12.1	
100	0.02	0.12	

of ions into mesopores on the electrode surface (see Fig. 2d), even though the electrode has a relatively high hydrophobic property.

Until now, it has been known that the micropore does not provide any effective mass transfer for ion adsorption and desorption because of overlapping effects (Farmer et al., 1996; Ying et al., 2002). Recently, however, Chmiola et al. reported that micropore less than 1 nm significantly increased the capacitance, thus optimized pore structures are required for highly improved performance in electrical and pulsative applications (Chmiola et al., 2006, 2008; Largeot et al., 2008). In addition, Avraham et al. obtained the ion selective carbon electrode by manipulating the size of the pore opening to the range of between monovalent and divalent ions (Avraham et al., 2008). Therefore, not only high surface area and capacitance, but also highly accessible pore size and harmonious structure of micropore and mesopore are required for efficient water softening (Wang et al., 2008). In addition, adequate pore size distribution between micropore and mesopore would be preferable for promising enhancement in efficiency.

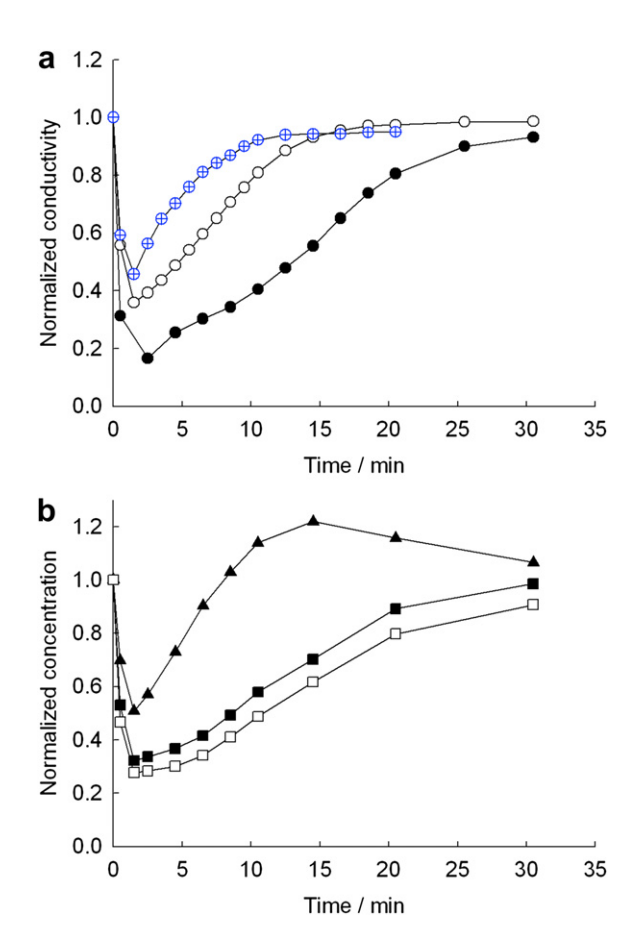


Fig. 5 – Effects of flow rates on removal of conductivity (a): 2 (\bullet), 4 (\circ), and 8 (\oplus) mL min⁻¹. Normalized concentration of ions (b): Na (\blacktriangle), Mg (\blacksquare), and Ca (\square) at a flow rate of 4 mL min⁻¹ using the AC cloth type electrode. The applied voltage was 1.5 V with the feed solution of 1000 μ S cm⁻¹ conductivity. The apparent surface area of each compartment was 25 cm².

3.2. Selective removal of ions

The effects of flow rates on the conductivity of product solution are shown in Fig. 5a. Flow rates were varied from 2 to 8 mL min⁻¹. The lowest conductivity of product solution was obtained at the flow rate of 2 mL min⁻¹ as almost 85% of removal efficiency after 2 min of operation. And then, the conductivity linearly increased. At the flow rate of 8 mL min⁻¹, only 55% of removal efficiency was obtained with a rapid increase of conductivity. These results indicate that the lower flow rates, the lower product conductivity is obtained due to high residual time of the solution inside the cells. However, although the lower flow rate has advantages on its low product conductivity, it is difficult to obtain high flux of the product solution. Thus, optimized flow rate is required depending on its applications.

Generally, in case of ion exchange process, it is well known that larger ions, i.e., smaller hydrated radius, and higher valence ions are more effectively removed (Park et al., 2007a). The ionic radius and valence of each ion are listed in Table S2. The preferential ion sorption for alkali and alkaline-earth metals are as follows:

$$Ca > Mg > K > Na \tag{1}$$

Interestingly, previous studies in CDI showed two contrary results on selective removal of ion species. Gabelich et al. reported that monovalent ions are preferentially removed than divalent ions (Gabelich et al., 2002), while different results were obtained by several researchers (Johnson and Newman, 1971; Gao et al., 2009; Xu et al., 2008). In the cases of Gabelich et al. and Xu et al., the carbon aerogel type electrode was used for ion adsorption and desorption. Even though they used carbon aerogel type electrodes, it seems that pore size and structure of each electrode would be different, exhibiting the opposite trends in preferential adsorption. It is reported that both pore size and structure of the electrodes has critical effects on removal efficiency of ions. Small size of pore attributed to selective adsorption of monovalent ions by reducing the pore size between the hydrated radius of monovalent ions (4 Å in diameter) and that of divalent ions (6–7 Å in diameter). The controlled pore range prohibited penetration of largely hydrated divalent ions into the pore (Avraham et al., 2008). In addition, another reason for the discrepancy could be the concentration of ions, which plays an important role in multi-ionic solution (Xu et al., 2008). Thus, optimized pore size and structure of an electrode are strongly recommended for selective removal of divalent ions in water softening applications.

The ion analysis result at the flow rate of 4 mL min⁻¹ is shown in Fig. 5b. The maximum removal efficiency of Ca is 73% with rapider increasing slope than the flow rate of 2 mL min⁻¹. In all cases, higher removal efficiency of Ca and Mg was obtained than Na (Supplemental Information, Fig. S3). Accordingly, we assume that the carbon cloth has appropriate pore size and structure for penetration of divalent ions into the electrode, resulting in a higher removal efficiency of the divalent ions. Additionally, the lower removal efficiency of Na, even higher relative conductivity than 1, would be due to a substitution of the adsorbed Na ions by Ca and Mg, which would be related with the ion selectivity (Figs. 5b, 6b and S3).

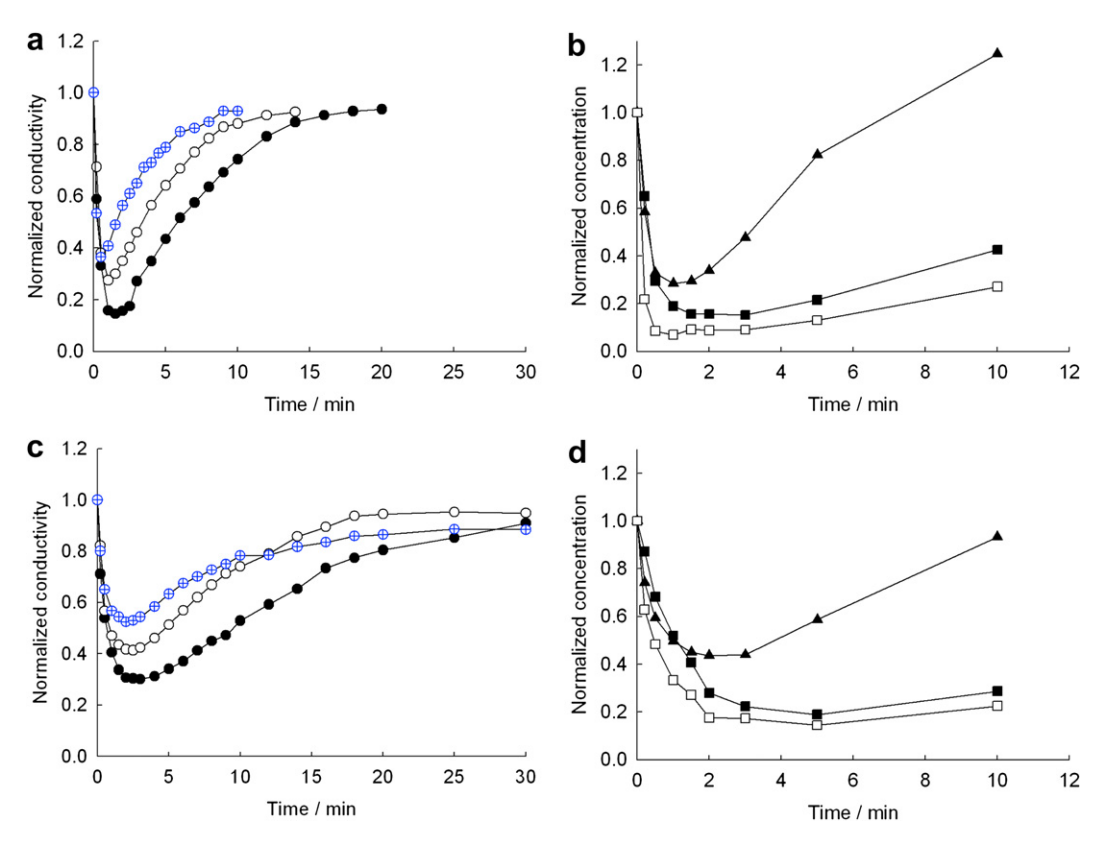


Fig. 6 – Effects of flow rates on removal of conductivity using (a) one sheet and (c) two sheets of the AC cloth electrodes: 16 (\bullet), 24 (\circ), and 32 (\oplus) mL min⁻¹. Normalized concentration of ions using (b) one sheet and (d) two sheets of the electrodes at a flow rate of 16 mL min⁻¹: Na (\blacktriangle), Mg (\blacksquare), and Ca (\square). The applied voltage was 1.5 V with the feed solution of 1000 μ S cm⁻¹ conductivity. The apparent surface area of each compartment was 100 cm².

In case of the ion exchange as described above, preferential removal of divalent ions is observed. In case of CDI, similarly, when the hydrated cations are electrically adsorbed on a negatively charged carbon electrode, highly charged divalent ions with smaller hydrated radius would be more strongly attracted. Furthermore, one research also supports the substitution of the ions in which competitive adsorption was observed over another species (Lee et al., 2008). Up to now, in CDI, almost no research has been focused on the substitution of the adsorbed Na by divalent ions in the authors' knowledge. Thus, it should be further investigated for appropriate understanding and interpretation.

Prior to a preparation of a five-cell stack, the apparent surface area of a unit cell was increased to 100 cm² at each compartment. The effects of flow rates on product conductivity and ion removal efficiency are shown in Figs. 6a,b, respectively. At a relatively low flow rate of 16 mL min⁻¹, the conductivity decreased to 15% of the initial value. Higher flow rates of 24 and 32 mL min⁻¹ exhibited lower removal efficiency in conductivity and shorter time for saturation, which are similar with previous results of 25 cm² unit cell. In case of the 16 mL min⁻¹, above 80% of Ca was removed for 10 min and slightly lower removal efficiency of Mg was obtained than that of Ca. Based on the results of the 100 cm² unit cell, no significant decrease in the removal efficiency was observed.

In order to increase total adsorption capacity, two sheets of carbon cloth were employed at each compartment, i.e., the two sheets of electrodes were piled. Thus thickness of the two piled electrodes was increased to two times while the apparent electrode area was maintained. As shown in Fig. 6c, the total adsorption time increased to 150-200% compared to the case in which one sheet of carbon cloth was employed at each compartment. Although the total effective adsorption time increased, the conductivity slightly decreased at the initial operation time within 5 min. It is assumed that the total resistance of electrodes also increased to two times because of the additionally employed carbon electrodes (series resistance). In Ohm's law, the increased resistance causes a voltage drop (V = IR), thus lowering actually applied voltage on both electrodes. It is well known that a low potential at both ends affects lower removal efficiency (Farmer et al., 1996; Lee et al., 2006). After optimization of the operation condition by further examination, this method would contribute to extended operation time as well as increased removal efficiency with the same apparent electrode area.

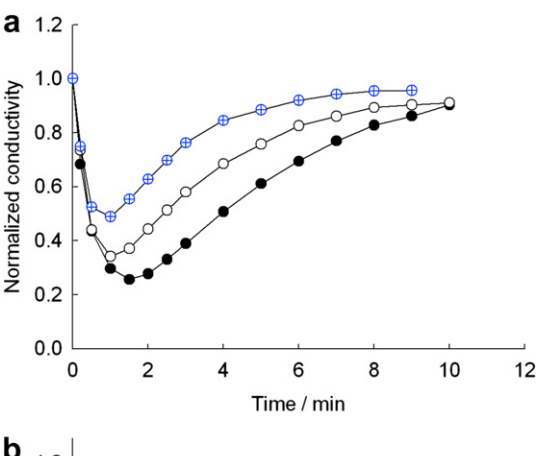
Effects of the two sheets of electrodes on removal of each ion are shown in Fig. 6d. About 80% of Mg and Ca ions were removed after 3 min of operation at the flow rates of 16 mL $\rm min^{-1}$. And then, the relative concentration of Mg and Ca were almost maintained within 10 min, while the relative concentration of Na more rapidly increased. In case of the flow rate of

24 mL min⁻¹, especially, higher removal efficiency of Ca (about 90%) was obtained after 3 min of operation (Supplemental Information, Fig. S4). Similarly, relative concentration of Na rapidly increased to above 1. Thus, the selective adsorption of those divalent ions compared to the monovalent ion was also observed regardless of electrode amount.

In order to prepare a CDI stack for higher treatment capacity, five pairs of cells were constructed with an each effective cell area of 100 cm² (total 500 cm²). As can be seen in Fig. 7a, relatively lower flow rate of 80 mL min⁻¹ showed the lowest product conductivity as 25% of the initial conductivity. Similarly, Fig. 7b showed higher removal efficiency of Ca and Mg than that of Na at the flow rate.

Cyclic tests of operation and regeneration were performed for the evaluation of CDI applicability (Fig. 8). For the purpose of continuous treatment with a flow rate of 120 mL min⁻¹, 4 and 1 min of operation and regeneration time were selected, respectively, based on the previous results. In the regeneration process, the flow rate was also fixed at 120 mL min⁻¹.

During the operation process, low conductivity of the product solution was obtained. During the regeneration process, on the other hand, 2.5 times higher conductivity than that of the initial feed solution was obtained due to the



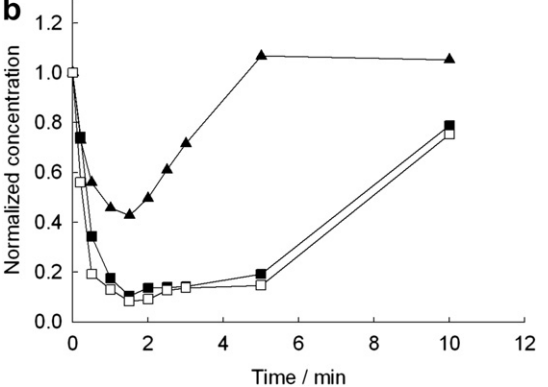


Fig. 7 – (a) Effects of flow rates on removal of conductivity using the AC cloth type electrode: 80 (\blacksquare), 120 (\bigcirc), and 160 (\boxplus) mL min⁻¹. (b) Normalized concentration of ions at a flow rate of 80 mL min⁻¹ using the AC cloth type electrode: Na (\blacktriangle), Mg (\blacksquare), and Ca (\square). The applied voltage was 1.5 V with the feed solution of 1000 μ S cm⁻¹ conductivity. The apparent surface area of each compartment in five-cell stack was 100 cm².

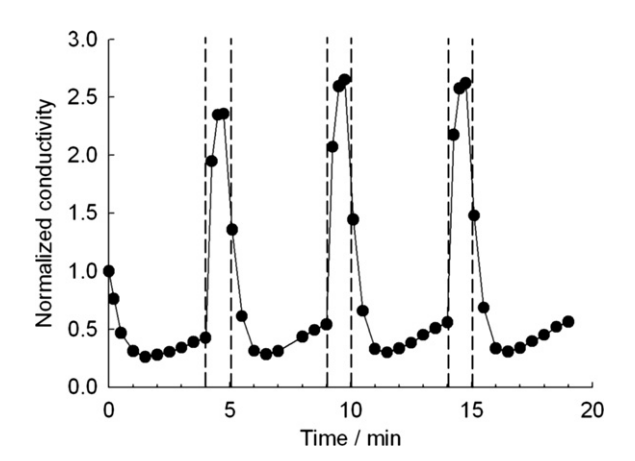


Fig. 8 – Cyclic tests with the five-cell stack in which the AC cloth type electrodes were employed. The operation process was conducted for 4 min and regeneration process was conducted for 1 min. The applied voltage was 1.5 V with the feed solution of 1000 $\mu S \ cm^{-1}$ conductivity. The apparent surface area of each compartment in the five-cell stack was 100 cm².

extracted ions from the electrical double layers in both electrodes. In order to achieve better regeneration efficiency, an inverse voltage was applied for 15 s, resulting rapid desorption of ions by repelling forces to them. And then, 0 V was maintained for the remaining 45 s to prevent adsorption of the detached ions at each opposite electrode.

3.3. CDI cell characterization

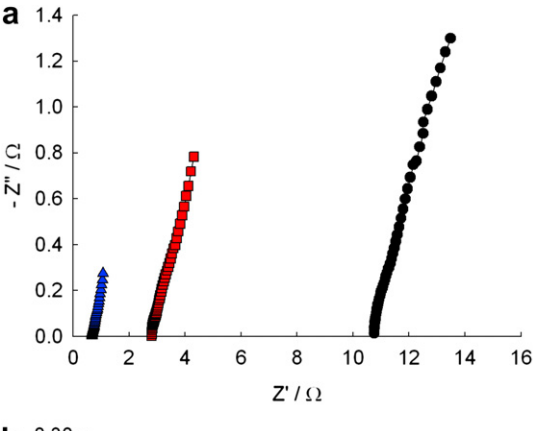
Impedance variations in the unit cell according to operational conditions are shown in Fig. 9. This Nyquist plot shows real (horizontal axis, Z') and imaginary (vertical axis, Z'') impedances depending on each frequency. The Nyquist plot of a CDI system can be analyzed using the equivalent circuit shown in Fig. 10. Impedance (Z) of an electrochemical system excluding the Warburg impedance is described as follows (Bard and Faulkner, 2001; Park et al., 2006; Largeot et al., 2008):

$$Z(\omega) = \left(R_{E} + \frac{R_{p}}{1 + \omega^{2}R_{p}^{2}C_{d}^{2}}\right) - j\left(\frac{\omega R_{p}^{2}C_{d}}{1 + \omega^{2}R_{p}^{2}C_{d}^{2}}\right)$$
(2)

where R_E is resistance of carbon electrode and electrolyte solution, R_p is the polarization resistance, C_d is the double layer capacitance, and $\omega=2\pi f$ (f is the frequency). At very high frequencies (1 $\ll \omega$), the Warburg impedance, which represent a kind of resistance for mass transfer, becomes unimportant, and then the total impedance becomes,

$$Z(\omega) \cong \left(R_E + \frac{1}{\omega^2 R_p C_d^2}\right) - j\left(\frac{1}{\omega C_d}\right) \cong R_E$$
 (3)

This impedance at high frequency ranges mostly represents the resistance of electrolyte solution and carbon electrode, which are responsible for the faradaic process in the unit cell. In case of the CDI process, this electrolyte resistance is inversely related with concentration of ionic species. It means that a higher concentration of ions in electrolyte solution shows lower resistance of the solution, and vice versa.



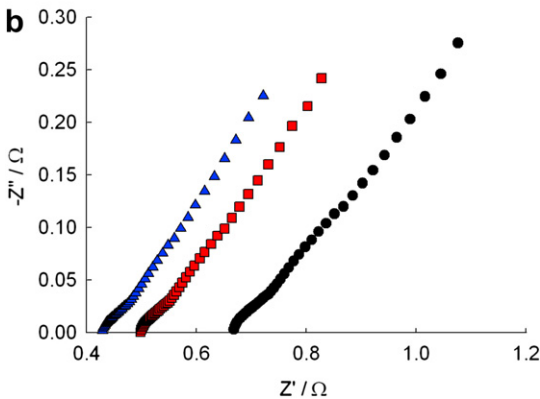


Fig. 9 – Impedance spectra of the CDI unit cell depending on (a) solution types: D.I. water (●), feed water (■), and after disconnection (△), and (b) cell voltages after disconnection from the power supply: 1.0 (●), 0.8 (■), and 0.6 (△) V. The apparent surface area of each compartment was 25 cm².

As shown in Fig. 9a, firstly, deionized water (\bullet) was injected to the cell after several tests, showing the highest resistance of 10.8 Ω due to the high resistance of the injected deionized water. And then, the feed solution (\blacksquare) was injected without any applying potential, showing lowered resistance of 2.8 Ω . Finally, after the CDI operation at 1.5 V, the cell was disconnected from the power supply, and then intentionally short-circuited (\triangle) in the existence of the feed solution. Adsorbed ions on each electrode gradually diffused into the bulk feed solution, thus, the concentration of ionic species

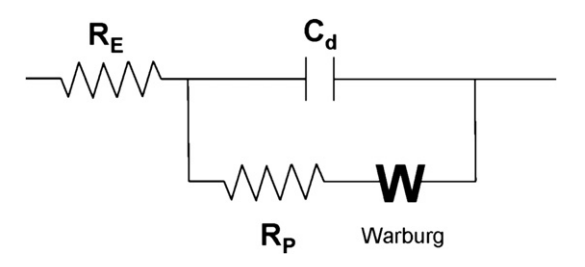


Fig. 10 – Equivalent circuit for the CDI system used in this study. $R_{\rm E}$: resistances of carbon electrodes and electrolyte solution, $R_{\rm p}$: polarization resistance, $C_{\rm d}$: double layer capacitance, and W: Warburg impedance.

increased more than the feed solution, and cell resistance decreased to 0.67 Ω . Thus, the shift from right to left at the left intercept of each impedance represent the decrease in electrolyte resistance due to higher ionic concentration depending on each operational condition.

As the frequency approaches to lower ranges, the double layer capacitance (C_d), polarization resistance (R_p), and Warburg element (W) are getting important. The C_d arises due to the interface between carbon electrodes and electrolyte solution, forming the Helmholtz plane (Oren, 2008) as well as contacts of electrodes. The R_p is related with a charge transfer resistance between the polarizable carbon electrode and electrolyte solution in which electric and ionic charging occur, respectively. The Warburg element refers to diffusion-controlled mass transfer effects at the interface, resulting in a linear slope.

After the CDI operation, the cell was disconnected from the power supply, and then discharged by short-circuiting both electrodes (Fig. 9). Open circuit voltage of the cell decreased from 1.0 to 0.6 V by losing polarity of each electrode. At the same time, the adsorbed ions were diffused into bulk solution due to the lowered polarity, thus concentration of ion species in the bulk solution increased. At a high frequency range, as a result, the measured resistance decreased, which is consistent with the above results shown in Fig. 9a. However, as the $R_{\rm E}$ was varied at different conditions, characteristics of the $C_{\rm d}$, $R_{\rm p}$, and W exhibited no significant effects with similar semi-circles and linear slopes.

4. Conclusions

- A highly wettable electrode is more effective for continuous treatment system due to fast adsorption/desorption rates.
- For applications of water softening, it is needed to have appropriate pore size and structure with highly accessible mesopores and branched micropores.
- During continuous CDI operation, higher removal efficiency
 of Ca and Mg was observed rather than Na. Furthermore,
 substitution of Na by divalent ions was observed due to
 a higher selectivity of the divalent ions.

Appendix A. Supplemental material

Supplementary information for this manuscript can be downloaded at doi: 10.1016/j.watres.2009.10.020.

REFERENCES

Ahn, H.-J., Lee, J.-H., Jeong, Y., Lee, J.-H., Chi, C.-S., Oh, H.-J., 2007. Nanostructured carbon cloth electrode for desalination from aqueous solutions. Mater. Sci. Eng. A-Struct. Mater. Prop. Microstruct. Process 449-451, 841-845.

Avraham, E., Yaniv, B., Soffer, A., Aurbach, D., 2008. Developing ion electroadsorption stereoselectivity, by pore size adjustment with chemical vapor deposition onto active carbon fiber electrodes. Case of Ca²⁺/Na⁺ separation in water capacitive desalination. J. Phys. Chem. C 112, 7385–7389.

- Bard, A.J., Faulkner, L.R., 2001. Electrochemical Methods: Fundamentals and Applications. John Wiley & Sons, NJ.
- Chmiola, J., Yushin, G., Gogotsi, Y., Portet, C., Simon, P., Taberna, P.L., 2006. Anomalous increase in carbon capacitance at pore sizes less than 1 nanometer. Science 313, 1760–1763.
- Chmiola, J., Largeot, C., Taberna, P.L., Simon, P., Gogotsi, Y., 2008. Desolvation of ions in subnanometer pores and its effect on capacitance and double-layer theory. Angew. Chem. Int. Ed. 47, 3392–3395.
- Čuda, P., Pospíšil, P., Tenglerová, J., 2006. Reverse osmosis in water treatment for boilers. Desalination 198, 41–46.
- Farmer, J.C., Fix, D.V., Mack, G.V., Pekala, R.W., Poco, J.F., 1996. Capacitive deionization of NaCl and NaNO₃ solutions with carbon aerogel electrodes. J. Electrochem. Soc. 143, 159–169.
- Gabelich, C.J., Tran, T.D., Suffet, I.H., 2002. Electrosorption of inorganic salts from aqueous solution using carbon aerogels. Environ. Sci. Technol 36, 3010–3019.
- Gabrielli, C., Maurin, G., Francy-Chausson, H., Thery, P., Tran, T.T. M., Tlili, M., 2006. Electrochemical water softening: principle and application. Desalination 201, 150–163.
- Gao, Y., Pan, L., Li, H., Zhang, Y., Zhang, Z., Chen, Y., Sun, Z., 2009. Electrosorption behavior of cations with carbon nanotubes and carbon nanofibres composite film electrodes. Thin solid films 517, 1616–1619.
- Ghizellaoui, S., Chibani, A., Ghizellaoui, S., 2005. Use of nanofiltration for partial softening of very hard water. Desalination 179, 315–322.
- Johnson, A.M., Newman, J., 1971. Desalting by means of porous carbon electrodes. J. Electrochem. Soc. 118, 510–517.
- Largeot, C., Portet, C., Chmiola, J., Taberna, P.L., Gogotsi, Y., Simon, P., 2008. Relation between the ion size and pore size for an electric double-layer capacitor. J. Am. Chem. Soc. 130, 2730–2731.
- Lee, J.-B., Park, K.-K., Eum, H.-M., Lee, C.-W., 2006. Desalination of a thermal power plant wastewater by membrane capacitive deionization. Desalination 196, 125–134.
- Lee, D., Ko, E.-Y., Lee, H.C., Kim, S., Park, E.D., 2008. Adsorptive removal of tetrahydrothiophene (THT) and tertbutylmercaptan (TBM) using Na-Y and AgNa-Y zeolites for fuel cell applications. Appl. Catal. A-Gen 334, 129–136.

- Oren, Y., 2008. Capacitive deionization (CDI) for desalination and water treatment past, present and future (a review). Desalination 228, 10–29.
- Park, J.-S., Choi, J.-H., Woo, J.-J., Moon, S.-H., 2006. An electrical impedance spectroscopic (EIS) study on transport characteristics of ion-exchange membrane systems. J. Colloid Interface Sci. 300, 655–662.
- Park, J.-S., Song, J.-H., Yeon, K.-H., Moon, S.-H., 2007a. Removal of hardness ions from tap water using electromembrane processes. Desalination 202, 1–8.
- Park, K.-K., Lee, J.-B., Park, P.-Y., Yoon, S.-W., Moon, J.-S., Eum, H.-M., Lee, C.-W., 2007b. Development of a carbon sheet electrode for electrosorption desalination. Desalination 206, 86–91.
- Schulze, M., Lorenz, M., Kaz, T., 2002. XPS study of electrodes formed from a mixture of carbon black and PTFE powder. Surf. Interface Anal 34, 646–651.
- Seaton, N.A., Walton, J.P.R.B., Quirke, N., 1989. A new analysis method for the determination of the pore size distribution of porous carbons from nitrogen adsorption measurements. Carbon 27, 853–861.
- Wang, J., Yang, X., Wu, D., Fu, R., Dresselhaus, M.S., Dresselhaus, G., 2008. 2008. The porous structures of activated carbon aerogels and their effects on electrochemical performance. J. Power Sources 185, 589–594.
- Welgemoed, T.J., Schutte, C.F., 2005. Capacitive deionization technology(TM): an alternative desalination solution. Desalination 183, 327–340.
- Xu, P., Drewes, J.E., Heil, D., Wang, G., 2008. Treatment of brackish produced water using carbon aerogel-based capacitive deionization technology. Water Res. 42, 2605–2617.
- Yang, K.-L., Yiacoumi, S., Tsouris, C., 2003. Electrosorption capacitance of nanostructured carbon aerogel obtained by cyclic voltammetry. J. Electroanal. Chem. 540, 159–167.
- Ying, T.-Y., Yang, K.-L., Yiacoumi, S., Tsouris, C., 2002. Electrosorption of ions from aqueous solutions by nanostructured carbon aerogel. J. Colloid Interface Sci. 250, 18–27.
- Zou, L., Morris, G., Qi, D., 2008. Using activated carbon electrode in electrosorptive deionisation of brackish water. Desalination 225, 329–340.